New Journal of Physics
An Institute of Physics and Deutsche Physikalische Gesellschaft Journal

Quantum optics with single quantum dot devices

Valéry Zwiller[1], **Thomas Aichele**[2] **and Oliver Benson**[2,3]

[1] Institute of Quantum Electronics, ETH, CH-8093 Zürich, Switzerland
[2] Nano-Optics, Physics Department, Humboldt University, D-10117 Berlin, Germany
E-mail: zwiller@phys.ethz.ch

New Journal of Physics **6** (2004) 96
Received 13 February 2004
Published 29 July 2004
Online at http://www.njp.org/
doi:10.1088/1367-2630/6/1/096

Abstract. A single radiative transition in a single-quantum emitter results in the emission of a single photon. Single quantum dots are single-quantum emitters with all the requirements to generate single photons at visible and near-infrared wavelengths. It is also possible to generate more than single photons with single quantum dots. In this paper we show that single quantum dots can be used to generate non-classical states of light, from single photons to photon triplets. Advanced solid state structures can be fabricated with single quantum dots as their active region. We also show results obtained on devices based on single quantum dots.

[3] Author to whom any correspondence should be addressed.

PII: S1367-2630(04)76177-7

Contents

1. Introduction

Quantum optics experiments with nanostructures enable the generation of single photons as well as photon pairs and photon triplets. Because nanostructures can be engineered at will in terms of material composition and shape, their emission properties can be tailored. Moreover, advanced structures can be fabricated with single nanostructures as their active elements. Structures where the emission is induced by electrical injection or where the photon emission is defined by a microcavity have been realized.

In this paper, we will first give a short overview of various physical systems that have been demonstrated to be single-photon sources on demand in section 2. We will then dwell on self-assembled Stranski–Krastanow grown quantum dots in more details in section 3. Optical spectroscopy of quantum dots is the main tool to understand the physics of quantum dots, very similar to atoms a century ago. Studying quantum dots at the single-dot level enables us to

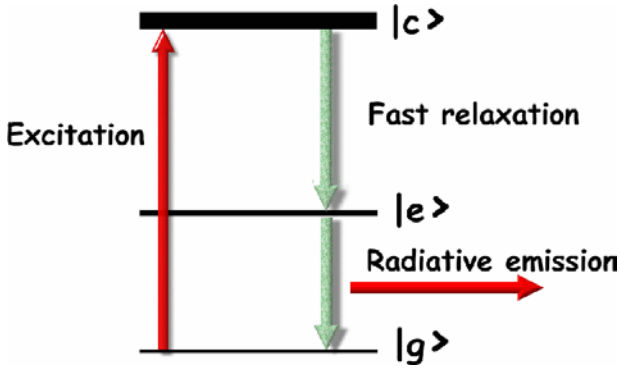

Figure 1. Schematic energy levels of a quantum emitter for single-photon emission.

escape from the statistical or inhomogenous broadening inherent in the study of quantum-dot ensembles. Section 4 will be devoted to single quantum dot spectroscopy and single-photon generation. The possibility to generate photon pairs as well as photon triplets on demand will be demonstrated in section 5. Devices based on single quantum dots are now being fabricated and we will report on single quantum dots grown on tips, single quantum dot light-emitting diodes and single quantum dots in microcavities in section 6. In section 7, we will give an overview of the current status of single-photon detectors where drastic improvements are currently being made by improving existing semiconductor technology or by developing completely novel devices based on superconducting nanostructures. Single-photon sources on demand have only been used for one application so far: quantum cryptography. A vast number of exciting applications and experiments will be explored as better single-photon sources are developed. We will point out some single-photon experiments in section 8 before concluding.

2. An overview of single-photon generation on demand with single-quantum emitters

It is possible to generate single photons by filtering the emission from a single transition in a single-quantum emitter. The quantum emitter may be a single atom, a single molecule, a single defect, or a single quantum dot. The principle of single-photon generation with single-quantum emitters is based on the excitation of the emitter followed by radiative emission, as shown in figure 1 and collection of the emission from a single emitter. Because the excitation does not need to be resonant with the radiative transition under study, filtering and collecting single photons is experimentally straightforward.

2.1. Single-photon demonstration: Hanbury-Brown and Twiss interferometry

A problem common to all single-photon-generation techniques is the demonstration that single photons are indeed being emitted. An answer to this problem lies in the photons' correlations. Photon correlations are used to demonstrate single-photon generation because no commercial detector currently available is able to resolve the number of photons. We will come back to this issue of detecting single photons in section 7.

Photon-correlation measurements consist in measuring the joint probability of detecting the arrival of a photon at time t and of another photon at time $t + \tau$. The normalized second-order

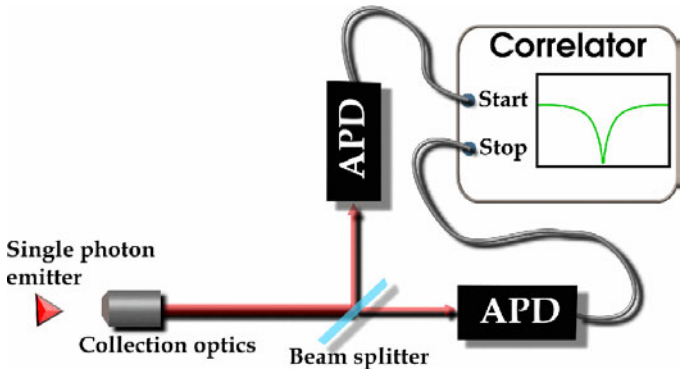

Figure 2. Schematic of a Hanbury-Brown and Twiss interferometer. A 50 : 50 beamsplitter sends the incoming beam towards two single-photon detectors (avalanche photo diodes). The signal from the detectors is fed into a correlator.

correlation function, the $g^{(2)}$ function which can be measured experimentally assuming a low photon detection probability is defined as

$$g^{(2)}(\tau) = \frac{\langle : I(t)I(t+\tau) : \rangle}{\langle I(t) \rangle \langle I(t+\tau) \rangle}. \tag{1}$$

This function can be measured with a Hanbury-Brown and Twiss interferometer [2] if the photon detection probability ρ is low. A rigorous treatment of the $g^{(2)}$ function is given by Scully and Zubairy [1]. We define the photon detection probability ρ as $\rho = \eta_{rad} T \eta_{det}$ where η_{rad} is the emitter quantum efficiency, T the probability for a photon to reach the detector and η_{det} the detector quantum efficiency.

For our purpose, a Hanbury-Brown and Twiss interferometer consists of two photon detectors able to detect single photons, a 50 : 50 beam splitter and correlation electronics that measure the time delay between detection events in the two detectors, see figure 2.

After a large number of events have been recorded, a histogram of the time intervals can be plotted. In the case of coherent light, a flat line with Poissonian fluctuations will be observed. In the case of single photons, a dip referred to as the 'antibunching dip' will be visible around $\tau = 0$ as seen in figure 3. This dip shows that two photons are less likely to be detected simultaneously than within large time intervals. Ideally, the antibunching dip goes down to zero at $\tau = 0$, which demonstrates that single photons are being generated, as there are never two photons entering the interferometer simultaneously.

Simple statistical considerations show that a single-photon emitter will yield a dip down to zero, while two single-photon emitters will yield a dip down to a normalized value of 0.5 and n single-photon emitters will yield a dip down to $1 - (1/n)$. A photon correlation measurement is therefore a tool to count a small number of single-photon emitters. The width of the antibunching dip is set by the cycling time of the emitter, it amounts to the time taken by the excited emitter to decay radiatively and to be excited again. Under weak excitation, it will therefore amount to a lifetime measurement, although the excitation is continuous. As the excitation power is increased, the antibunching dip will become narrower because immediate reexcitation following photon emission is likely to take place. The dip can be fitted with an equation of the form

$$correlations\ (t) = A[1 - \mathrm{e}^{-(t/\tau_{re})}], \tag{2}$$

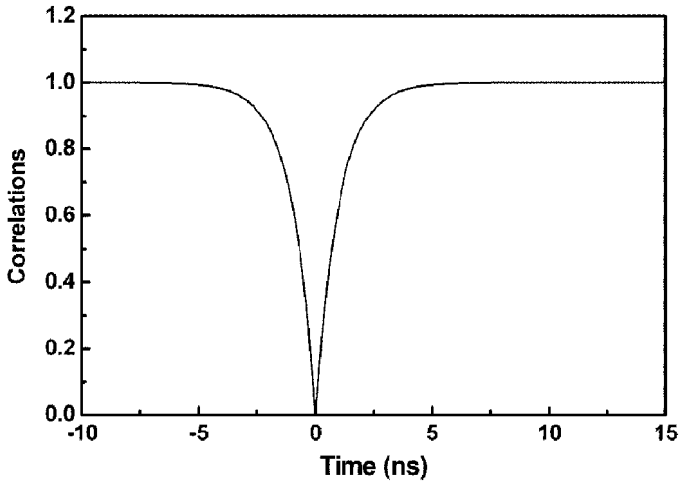

Figure 3. $g^{(2)}$ function for a single-photon emitter under continuous excitation.

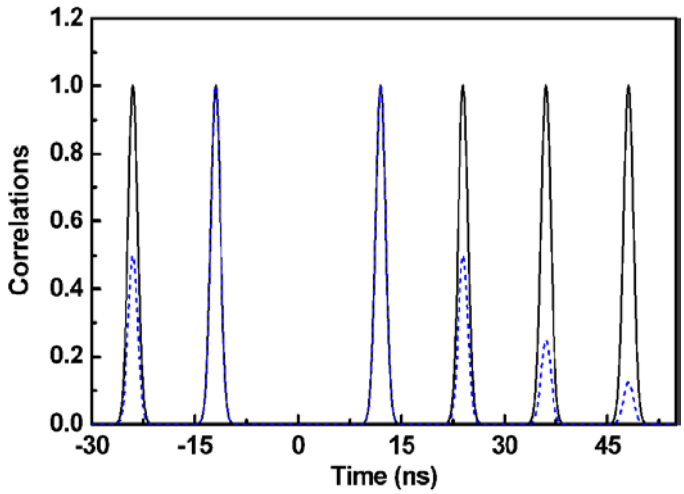

Figure 4. Photon correlation function for a single-photon emitter under pulsed (80 MHz repetition rate) excitation. The solid line represents the case of weak detection probability. The dashed blue line represents the case where the detection probability ρ is 0.5.

where A is a normalization factor and τ_{re} is the system recycling time. The time resolution of the detectors and of the correlation electronics must be short compared to the lifetime of the transition under study, otherwise the measured antibunching dip will suffer from the convolution by the system time response and will not reach its optimal value.

The same experiment done under pulsed excitation, provided that the excitation pulse is much shorter than the radiative lifetime to avoid immediate re-excitation, amounts to single-photon generation on demand, where an excitation pulse (optical or electrical) will yield the emission of a single photon. Figure 4 shows ideal antibunched correlations for a single-photon emitter under pulsed excitation, with an 80 MHz excitation repetition rate. In these conditions, each excitation pulse generates one and only one photon with radiative decay of the quantum system. The peak at $\tau = 0$ should therefore completely vanish as it can only start the correlation

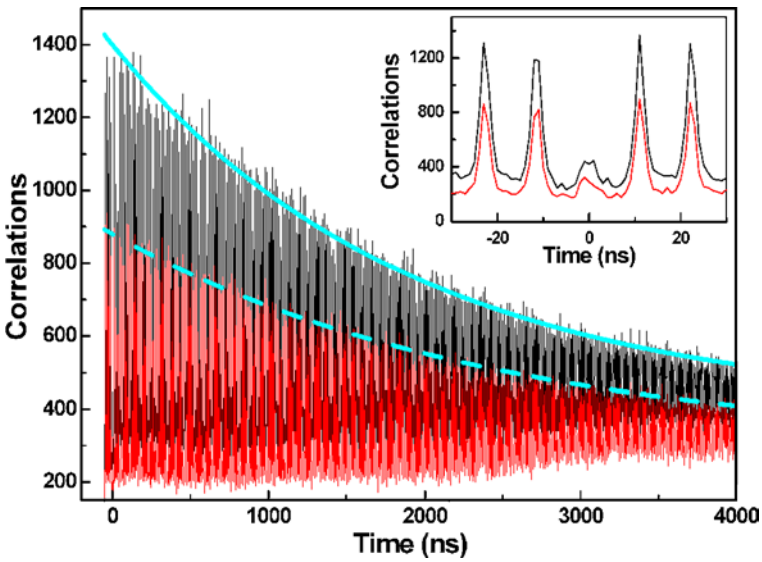

Figure 5. Photon correlations measured under pulsed excitation with two different collection efficiencies on the emission from a single InP quantum dot. The inset is a zoom around $t = 0$, the strongly reduced peak at $t = 0$ demonstrates the antibunched nature of the emission.

counter. We must wait at least for the next excitation pulse to register a stop photon. Here again, the width of the peaks is set by the radiative lifetime of the single emitter under study.

In the case where the detection probability ρ is high, the Hanbury-Brown and Twiss interferometry measurements will be different from the $g^{(2)}$ function. In an ideal experiment where all single photons are collected and detected ($\eta_{rad} = \eta_{det} = 1$), we have $T = 0.5$ (because of the beamsplitter) for each detector. This means that the probability that the stop detector detects a photon after the following excitation pulse is 0.5 and is T^n for the nth pulse. If the photon detection probability is high, an exponential tail in the correlation measurements will be observed, as shown in figure 4 with the dashed blue line.

We have performed photon correlation measurements on a single-photon emitter with a limited detection probability and repeated the measurement after inserting an optical density filter on the entrance of the Hanbury-Brown and Twiss interferometer to reduce the incoming photon flux by a factor of 3.16 (optical density 0.5). The experimental results are shown in figure 5 and clearly show a modification of the photon correlation envelope with decreasing detection probability in agreement with the experimental attenuation. The exponential fits in figure 5 are of the form $Ae^{-(t/\tau)}$ with $A = 1000$ and $\tau = 1900$ for the continuous line (no attenuation) and $A = 580$ and $\tau = 2400$ for the dashed line (with attenuation). The envelope of the correlation measurements is therefore an indicator of photon detection probability ρ. The measured value of ρ fits very well to an estimation of $T\eta_{det}$, implying $\eta_{rad} \approx 1$.

2.2. Single atoms

The first experimental observation of antibunching was performed on an atomic beam of Na atoms in 1977 by Kimble *et al* [26]. They observed the spontaneous emission from an atomic beam,

and obtained a dip in a photon correlation measurement. The first sub-Poissonian antibunching measurement was reported by Diedrich and Walther [44] in 1987 on single atoms in a trap. The advantages of single atoms as single-photon sources are that all atoms of a given isotope are exactly indistinguishable, there is no variation in the emission properties from atom to atom, unlike for solid-state emitters. The coherence length of the emission from isolated single atoms is Fourier limited, the decoherence mechanisms are well understood and atomic physics is one of the most refined areas of physics. The disadvantages of this technique are the rather bulky experimental setups required to trap and observe single atoms, making the technique hard to scale down and integrate into small practical devices. Van Baeyer gives an overview of atomic physics down to observation of single atoms [45].

2.3. Single molecules

The fluorescence from a single molecule is also expected to be antibunched. Optical studies of single molecules is a very active field of research at the confluence of physics, chemistry and biology. Single-photon generation is only one of many applications for single molecule studies [27]. The advantages of single molecules for single-photon generation on demand are that the emission is efficient even at room temperature, the light extraction and collection efficiency can be very high since high numerical aperture microscope objectives can be used to collect the fluorescence and molecules are usually imbedded in low-refractive-index materials. Molecules emitting at all wavelengths from the UV to the IR are available. Single molecules have been used to generate single photons [28]–[31]. Disadvantages of this technique are that molecules are usually unstable and optically active only for some minutes before bleaching. Blinking is also a common problem for single-molecule studies. Blinking and bleaching can also be observed on the correlation measurements [32]. The fluorescence emission at room temperature is broad and sharper emission requires low temperatures.

2.4. Single defects

A single optically active defect can also be used for single-photon generation. Although there is a vast number of optically active defects in solid-state materials, the only defects that have been used to date are nitrogen-vacancy (NV) centres in diamonds [33]–[35]. Their emission is centred at 637 nm at room temperature with an emission width of 120 nm. Other defects could also be used for single-photon generation, for instance single-carbon acceptors in GaAs would emit single photons at a wavelength of 790 nm [39] or arsenic antisites in GaAs would emit in the infrared at around 1.3 μm [41]. The advantages of NV centres are that the defects are very stable and devices with large number of positioned defects could in principle be fabricated. Disadvantages are the rather long radiative lifetimes of the order of 10 ns, limiting the maximum single-photon-emission rate.

2.5. Photon turnstile device

A photon turnstile device based on the tunnelling of electrons and holes in a semiconductor device was suggested by Imamoglu and Yamamoto [36, 37], it is based on the tunneling of electrons and holes in a GaAs–AlGaAs double-barrier mesoscopic p–i–n heterojunction driven by an alternating voltage source. An experimental implementation was realized by Kim *et al* [38]. The operation of the device requires extremely low temperatures and no photon correlation measurements were performed to confirm single-photon generation.

2.6. Single quantum dots

Several types of self-assembled quantum dots have now been demonstrated to be good single-photon sources. By playing with the material parameters, it is possible to tailor the emission properties, most notably the emission wavelength. Gérard and Gayral [40] suggested that single photons could be generated by filling a single quantum dot with many excited carriers and then filtering out the final exciton emission. Because the exciton emission takes place at a different energy than other recombinations, only the last photon emitted by the quantum dot is then used no matter what the initial population was. The advantages of single quantum dots are that their radiative quantum efficiency is very high, III–V quantum dots are fully compatible with well established semiconductor processing technology, single dots can be positioned in pn junctions to obtain electroluminescence and in microcavities to engineer the emission geometry and control the radiative lifetimes. The main inconvenience of single quantum dots as single-photon sources is that up to now low temperatures have been required to operate the devices. Single-photon generation on demand has been realized at temperatures in excess of 100 K by Mirin with InGaAs quantum dots in GaAs [42]. The photon extraction is also a problem for quantum dots as we will see in the next section.

3. Quantum dots

The original paper by Stranski and Krastanow [3] in 1938 suggested that growth of two materials with different lattice constants would result in the formation of islands instead of flat layers beyond a critical thickness. The first strain induced islands were reported by Goldstein *et al* [4] in 1985 where InAs islands were formed on GaAs. These islands can have sizes in the range of a few nanometers and can confine charge carriers both in the conduction band and in the valence band. The physical properties of these structures has been reviewed by Petroff *et al* [5].

A completely different kind of quantum dots, known as colloidal quantum dots are produced in solutions. These dots tend to suffer from blinking and bleaching, improvements in their stability is required if practical devices are to be built with these dots, their properties are currently closer to those of molecules than to those of Stranski–Krastanow quantum dots. It must be noted however that these colloidal dots were the first type of quantum dots used to generate single photons [43]. But because of the advantages of Stranski–Krastanow grown quantum dots, most research has concentrated on epitaxially grown quantum dots. However, one advantage of colloidal dots over epitaxially grown quantum dots is that they still emit efficiently at room temperature.

3.1. The photon extraction problem

We have seen that quantum dots are very efficient light emitters, but the high refractive index of III–V semiconductors means that only a tiny fraction of the emitted light can leave the sample. This problem of photon extraction efficiency has plagued the light-emitting diode industry for decades [53]. Total internal reflection occurs for a small angle in high refractive index materials, taking $n_2 = 3.5$ (which is the value for GaAs around 1 μm [54]) we obtain

$$\theta_{tir} = \sin^{-1}(1/3.5) = 17^{\circ}.$$

This means that all photons reaching the semiconductor surface with an incident angle greater than 17° to the normal will be reflected inwards and will not make it out of the device to our eyes

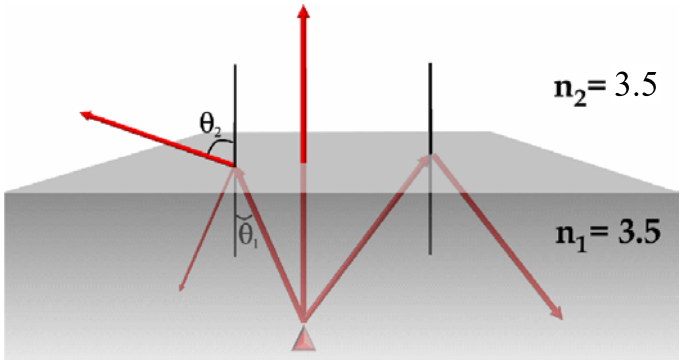

Figure 6. The photon extraction problem. The quantum dot is in a high-refractive-index medium (n_2); total internal reflection occurs for an incident angle of 17°.

or detectors as shown in figure 6. To find out the fraction of photons that leave the sample, we can calculate the cone of solid angle that makes it out of the material:

$$\Omega_c = 2\pi(1 - \cos\,\theta) = 2\pi\left(1 - \left(1 - \left(\frac{1}{2n^2}\right)\right)\right) = \frac{\pi}{n^2}\ \text{steradians}.$$

This has to be compared with 4π steradians:

$$\eta = \Omega_c/(4\pi) = \frac{1}{4n^2},$$

where η is the extraction efficiency. For $n = 3.5$, we get $\eta = 2\%$. We note here that these values are very optimistic as they assume that no photon with $\theta_1 \leqslant \theta_{tir}$ would be reflected; this would require a very elaborate antireflective coating.

3.2. Solid immersion lenses

Several techniques have been suggested to increase the light extraction efficiency: microcavities, solid immersion lenses (SILs) and surface plasmons [6]. Here, we will focus on SILs because of their broad transmission bandwidth, SILs can boost the extraction efficiency for a large range of wavelengths unlike for microcavities, enabling spectroscopy.

SILs were developed by Mansfield and Kino [7] to achieve higher optical resolutions and have been used to increase the spatial resolution of optical microscopes [8]. SILs are truncated dielectric spheres. We will see that SILs are also very useful to increase the light collection efficiency from single quantum dots and an improvement of more than an order of magnitude of the light extraction efficiency is feasible. An important advantage of SILs over other techniques is that SILs are broadband systems enabling efficient spectroscopic studies.

SILs discussed in the literature come in one of two designs, the hemisphere, and the Weierstrass (or superhemisphere) geometry as shown in figure 7. The hemisphere is particularly interesting in microscopy applications, since this lens gives no chromatic aberration (the light exits the SIL at normal incidence). This is useful for white light microscopy. In the Weierstrass geometry, the height of the SIL is $r + a = (1 + (1/n_2))r$, where n_2 is the refractive index of the SIL and r its radius as shown in figure 8. Weierstrass geometry has the added advantage that the emerging light is concentrated in a limited cone, further facilitating light collection.

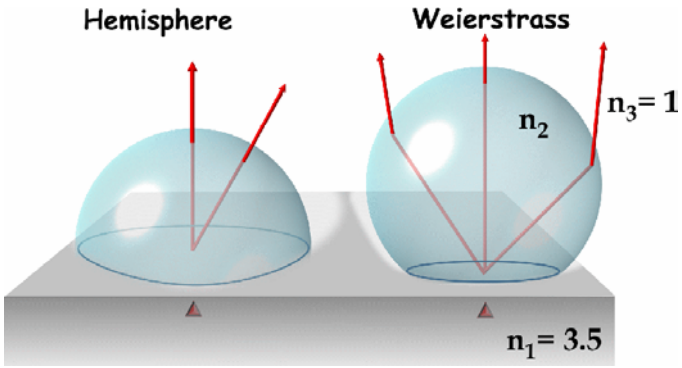

Figure 7. Solid immersion lenses are truncated dielectric spheres brought in contact with the sample and centred on the quantum dot under study. Left: hemisphere geometry. Right: Weierstrass geometry.

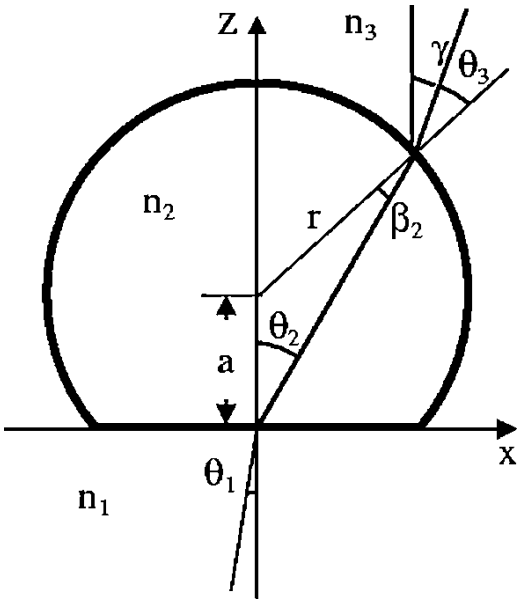

Figure 8. SIL geometry. The SIL has a radius r, a refractive index n_2 and is truncated at a height a below its centre.

We can express the photon exit angle γ from an SIL as a function of the entry angle θ_1 (the dispersion) for any truncated dielectric sphere:

$$\gamma = \arcsin\left[\frac{an_1}{rn_3}\sin(\theta_1)\right] - \arcsin\left[\frac{an_1}{rn_2}\sin(\theta_1)\right] - \arcsin\left[\frac{n_1}{n_2}\sin(\theta_1)\right] + \frac{\pi}{2}. \quad (3)$$

The extraction efficiency can be calculated with a Monte Carlo simulation based on equation (3). Figure 9 shows the expected extraction efficiency for Weierstrass SILs with a refractive index of 1.83 (LaSFN9 glass) and 3.5 (GaAs). We see that with a GaAs SIL, about 30% of the emitted light could be collected with collection optics with a numerical aperture of 0.3 and that increasing the numerical aperture would not increase further the collection efficiency. This is very relevant to low temperature micro-photoluminescence experiments, where the usually

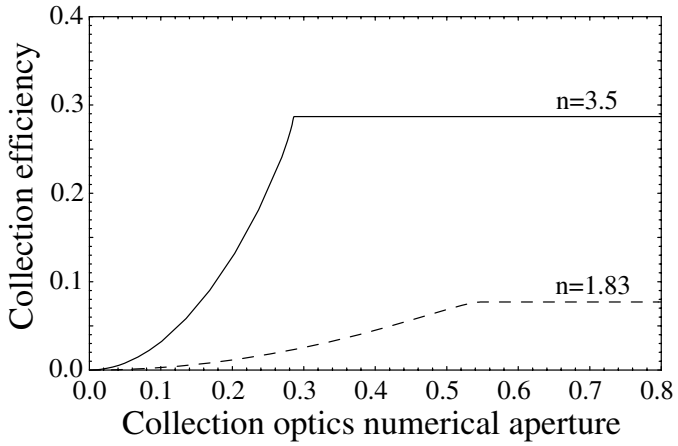

Figure 9. Extraction efficiency for the Weierstrass geometry calculated for two different SIL refractive indices: 3.5 (——) and 1.83 (– – –).

large spacing between the sample and objective prevents the use of high numerical aperture objectives.

Experiments have been done to compare the experimental extraction efficiencies from a single quantum dot with the calculated values. The same single quantum dot was measured under three conditions: without any SIL, with a hemisphere glass SIL, and with a Weierstrass glass SIL. The SIL was held onto the sample with a very thin layer of transparent wax, and in each case, the SIL was centred on the quantum dot with great care. The dot was also used as a laser power probe. The laser excitation power was adjusted so that the ratio of the biexciton to exciton peak was the same in all three experiments. This means that the dot was under the same excitation conditions in all three cases. The results are shown in figure 10. All spectra were taken with an objective with 0.4 numerical aperture and were normalized for each case. We see that with a hemisphere, the signal is 3.5 times stronger than without an SIL, and that the signal is nearly six times stronger when a Weierstrass SIL is used. This gain is particularly useful when photon correlations are measured. The number of correlations scales with the square of the incoming intensity. A gain in intensity by a factor of 6 will therefore result in 36 times more correlations.

It is also possible to directly form the SIL in the substrate using microfabrication techniques. Wet etching techniques can produce lens-shaped surfaces in III–V materials [77, 78]. Fabricating an SIL directly into the substrate would result in an SIL with the optimum refractive index, an antireflection layer would then further boost the collection efficiency. Placing a mirror below the quantum dot would further double the extraction efficiency. The surface roughness, the antireflection layers and the material absorption would then set the limit of the extraction efficiency.

4. Single-photon generation with different quantum dot systems

The key tool in single quantum-dot spectroscopy [79] is local probes to study the luminescence [80].

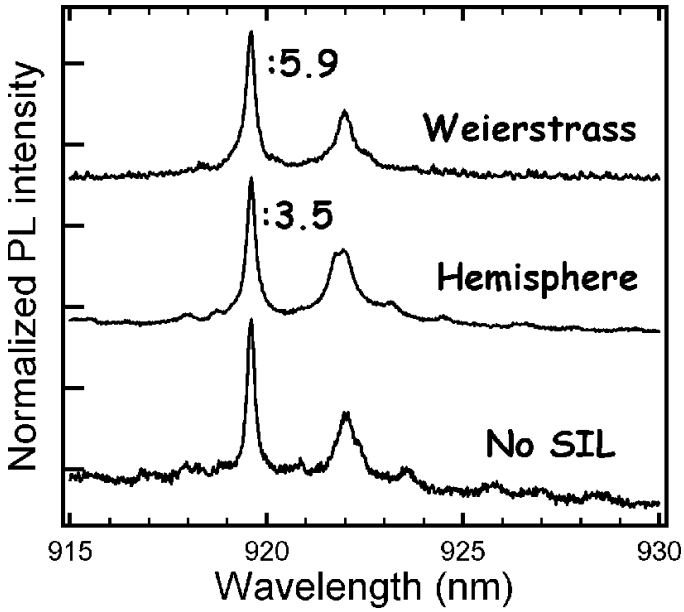

Figure 10. Light extraction efficiency measurements performed on the same single InAs/GaAs quantum dot with different SIL geometries with a refractive index of 1.83. The numbers indicate the peak intensity.

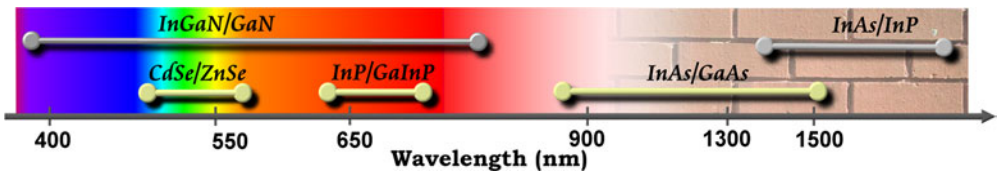

Figure 11. Schematic representation of the wavelength ranges accessible with different Stranski–Krastanow quantum dot material systems. The region inaccessible to silicon detectors is indicated by a brick wall.

In figure 11, we show a schematic representation of the wavelength emission ranges for several Stranski–Krastanow quantum dot-material systems. Up to now, single-photon generation has been achieved with the InAs/GaAs, InP/GaInP and CdSe/ZnSe quantum-dot systems.

The InAs/GaAs system is by far the most studied of all quantum-dot systems, emission is usually blue-shifted to enable detection with silicon detectors. Most work reported to date has been done on InAs dots emitting in the 900–950 nm range. Single dot spectroscopy has been performed at 1250 [70, 71] and 1300 nm [72] with this material system. Photon correlation measurements at these wavelengths will require good infrared single-photon detectors. Single-photon generation on demand at 1300 nm will be very useful for quantum cryptography with optical fibres. Quantum cryptography devices working at 1.3 μm with attenuated laser beams are already available on the market [73, 74].

InP dots in GaInP have been used to generate single photons in the 640–690 nm range [50] as well as photon pairs and triplets. This material system could in principle be used to generate single photons from 620 to 750 nm. The emission wavelength from these dots fits to the maximum efficiency of silicon avalanche photodiodes, a detection efficiency in excess of 70% can be reached at around 650 nm. This could be interesting for free space quantum cryptography

over moderate distances where the detectors' responses are more important than atmospheric transmission.

CdSe quantum dots in ZnSe have been used to generate single green photons at around 500 nm [64, 65]. One great advantage of this material system is its short radiative lifetime compared with III–V quantum dots, enabling the generation of single photons on demand with a small time uncertainty, suggesting that the maximum single-photon-emission rate can be much higher than for III–V dots [65]. This system also has a larger energy splitting between the exciton and the biexciton than for the InAs/GaAs material system. This larger splitting is useful to achieve a better filtering of the exciton emission, making operation at higher temperatures possible. The refractive index of ZnSe is lower than for GaAs, making the light extraction easier.

InGaN quantum dots imbedded in GaN have recently been studied at the single dot level [67, 69], and time-resolved measurements have been performed on the emission from single quantum dots [68]. This material system has the potential to cover the complete visible range, this might be useful for free-space quantum cryptography.

InAs dots imbedded in InP have been shown to be efficient emitters in the infrared [92], but no single dot optical studies have yet been reported for this material system. This material system could be used to generate single photons at 1.55 μm, where optical fibres have their lowest absorption.

Single quantum dots grown by techniques other than the Stranski–Krastanov growth mode have also been shown to emit single photons. Single InGaAs dots imbedded in AlGaAs with shapes and positions determined by the etching of pyramid-shaped holes in the substrate prior to the growth have been shown to emit single photons at a wavelength of 800 nm [81]. These pyramidal dots could emit over the range 750–870 nm. Single InAs quantum dots in GaAs wires have been reported to emit at 880 nm [82]. Fluctuations in GaAs quantum wells imbedded in AlGaAs have been used to generate single photons with very short lifetimes [83].

These material systems enable the generation of single photons at nearly any wavelength from the near-UV to the near-infrared, operation at higher temperatures will be possible by increasing the carrier confinement and the exciton–biexciton splitting.

5. *N*-photon generation with single quantum dots

We have seen that single quantum dots are well suited for single-photon generation through the filtering of the exciton decay. By modifying the experimental conditions, it is possible to generate other photon states. Photon pairs and photon triplets can be generated with single quantum dots through the cascaded recombination of multiexcitons into the ground state. Moreover, these cascade measurements enable an exact identification of the nature of the emission lines.

5.1. Photon pairs

Soon after exciton emission had been demonstrated to be antibunched, the biexciton emission was also shown to be antibunched [48, 49]. This enabled a beautiful experiment where the start and stop detectors in a Hanbury-Brown and Twiss interferometer would detect different transitions, each at a different energy. The result is an asymetric correlation demonstrating that the biexciton and exciton recombine successively. This was first performed on InAs/GaAs quantum dots [51, 52]. Green photon pairs have been generated with single CdSe/ZnSe quantum dots with

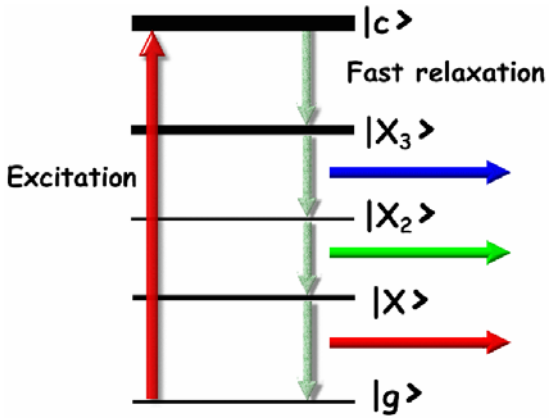

Figure 12. Schematics of energy levels of a three-photon cascade emitter. A triexciton will recombine yielding a biexciton and a photon, the biexciton will recombine to give an exciton and emit a photon.

the biexciton–exciton cascade [66]. In this experiment, polarization of the biexciton and exciton emissions were found to be collinearly polarized. These cross-correlation measurements are very useful to identify the biexciton emission from other transitions. Cross correlations can clearly demonstrate the sequentiality of emission from a single emitter.

5.2. Photon triplets

The idea of using both exciton and biexciton emissions to generate two photon states can easily be extended to the triexciton to generate photon triplets (figure 12). The main problem in this experiment is that, instead of a single triexciton emission line, a multitude of lines at widely different energies were obtained. Three-photon generation has been reported with InP quantum dots. Cross correlations on the triexciton, biexciton and exciton enable the exact identification of the emission lines.

6. Single quantum dot-based devices

Advanced processing technologies for III–V materials make it possible to fabricate complex structures with single quantum dots as the active region. We will present three types of devices based on single InP quantum dots imbedded in GaInP.

6.1. Single quantum dots on tips

Epitaxial growth of quantum dots is usually done on flat substrates. It is, however, interesting to perform quantum dot growth on patterned substrates. This enables one to control the position of the quantum dots. A good example is given by the growth of quantum dots in holes made in the substrate prior to growth [86, 88]. Dots can also be formed on tips [89, 87]. We have investigated the growth of InP quantum dots on etched tips in the GaAs substrate. Our aim is to fabricate sharp tips that would have a single dot at their apex. Such a device would be an interesting tool for quantum optics experiments. It would allow for apertureless near-field scanning optical

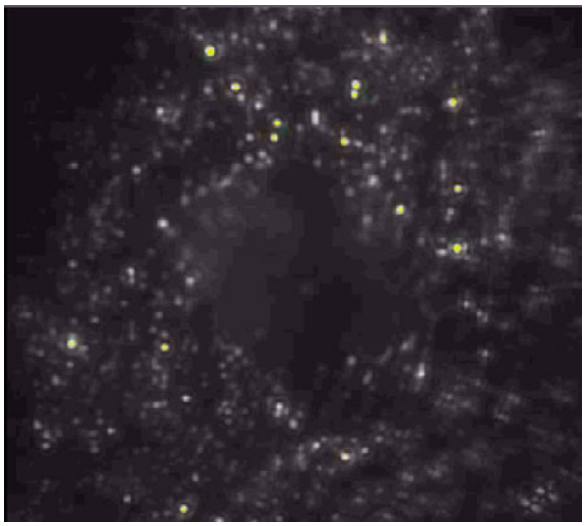

Figure 13. Microphotoluminescence movie of a tip with a few InP quantum dots. The movie was taken as the focal plane of the imaging optics was scanned up from the planar surface to the tip. (See animation.)

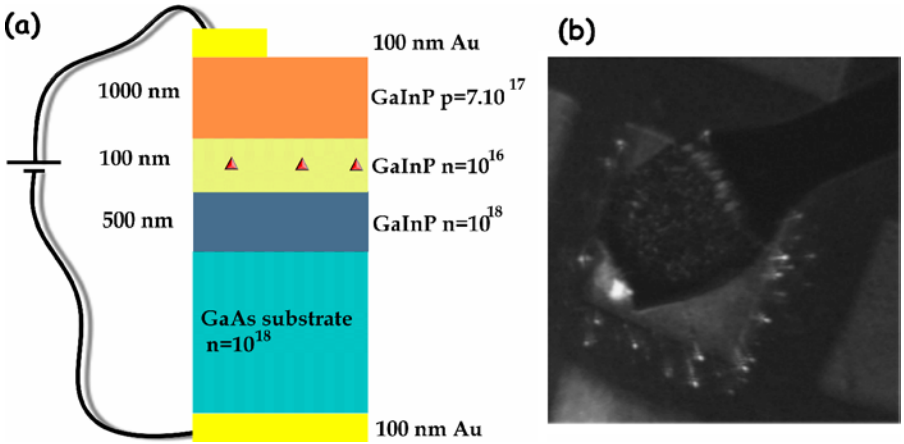

Figure 14. (a) Structure of the quantum-dot light-emitting diode. (b) Micro-electroluminescence image of single InP quantum dots.

microscopy as well as to couple the light from a single dot to high-Q microcavities. Because quantum dots do not bleach and rarely blink, the experiments that have been performed with single molecules on tips [31] could be done with a more stable system. Figure 13 shows a movie taken on a tip with a few quantum dots at its apex. The movie was taken by scanning the focal plane of the micro-photoluminescence set-up from the planar surface to the tip's apex.

6.2. Single quantum dot light-emitting diode

Positioning quantum dots in pn junctions enables the study of electroluminescence [90]. Figure 14(a) shows a quantum-dot light-emitting-diode structure that was grown by metal organic vapour phase epitaxy with a very low density of InP quantum dots in a pn junction. Figure 14(b)

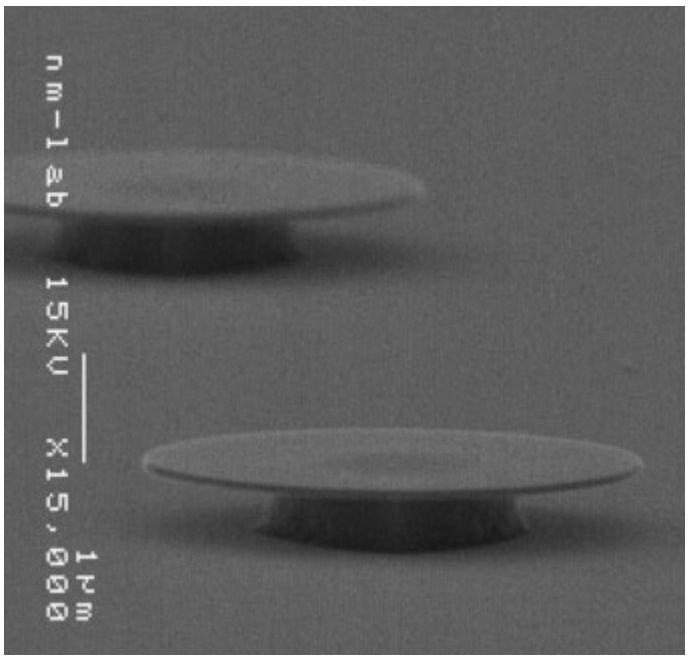

Figure 15. Scanning electron microscope image of a GaInP microdisk. The disk is 100 nm thick and 4 μm in diameter.

shows a micro-electroluminescence image taken at a temperature of 10 K under a forward bias of 3.5 V. Each bright spot is a single quantum dot. The sides of the square contact pad are of length 30 μm. This device presents the principle to obtain stable emission from the quantum dots: the dots should be imbedded in a thick intrinsic region.

6.3. Single quantum dots in microcavities

Optical microcavities confine light in small volumes and redefine the emission characteristics of imbedded emitters in terms of emission geometry and emission lifetime [91]. There are many different types of microcavities relying on different schemes to confine the photons.

One major problem which has been the source of debate is the positioning of the quantum dots in microcavities. Modifications of the emission properties must be correlated to the position of the dots in the microcavity to control all the parameters in these experiments. Different schemes have been implemented to position single quantum dots in microcavities relying either on optical mapping of the quantum dots prior to the fabrication of the microdisks or through the use of atomic force microscopy of thinly capped quantum dots to measure their position with great accuracy.

We have produced microdisks with a diameter of 4 μm and thickness of 100 nm using electron beam lithography and several wet etching steps. Figure 15 shows a GaInP microdisk containing a few InP quantum dots. Microdisks confine light at their edges in whispering modes and high Q-factors can be achieved in excess of 10 000.

We have also produced another type of microcavity where the light is confined in a pillar between two distributed Bragg reflectors. Figure 16(a) shows a wet-etched micropillar containing a few InP quantum dots. Figure 16(b) shows a micro-photoluminescence image of the same microcavity. A few randomly positioned dots are visible.

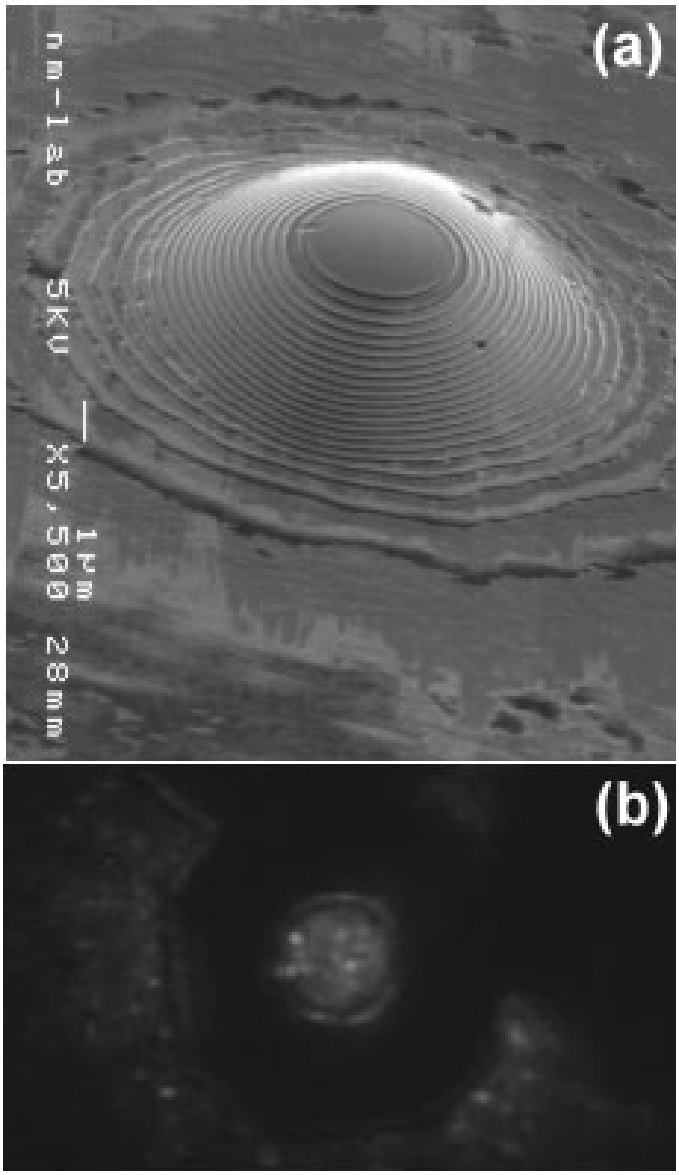

Figure 16. (a) Scanning electron microscope image of a wet etched micropillar containing InP quantum dots. (b) Micro-photoluminescence image of the structure after deposition of a top dielectric DBR. A few quantum dots are seen.

7. Single-photon detection

Detecting single photons with a high time resolution and low noise is also a challenge. Historically, photomultiplier tubes (PMTs) played a great role, but have been replaced by semiconductor avalanche photodiodes (APDs) in many single-photon detection experiments [55]. APDs offer very high quantum efficiencies with very low dark noise. The time resolution is a tradeoff with the noise level. PMTs still have an advantage over APDs when short time resolutions are required. Typical time resolutions achieved with silicon APDs are about 500 ps. At the cost of higher noise level, time resolution as short as 50 ps can be achieved with silicon

APDs. In the infrared, InGaAs and germanium APDs are available with much higher darkcounts and worse time resolutions than silicon APDs [57]–[60].

Devices based on superconducting nanostructures have recently been developed that are able to detect single photons. Two types of superconducting detectors are currently being developed: hot electron detectors with very fast response times and microcalorimeters that are able to resolve the number of photons in a pulse.

Hot electron detectors are based on thin stripes of NbN wires cooled below their critical temperature. The absorption of a single photon induces enough heating in the wire to break the superconductivity [93]–[98] and yields a measurable voltage spike. The main advantage of these detectors lies in their speed–time resolutions of 50 ps have been achieved and the dead time is of the order of 50 ps. Their darkcounts are a tradeoff with the quantum efficiency. Single photons can be detected far in the infrared. The bias also lets the device be sensitive to single photons or to photon pairs. Although these detectors do not count photons, they can be set to be sensitive to single photons or to photon pairs.

A device based on microcalorimeters has been demonstrated to be able to resolve the number of photons in a pulse [63]. Although this type of device is very slow, the ability to measure the number of photons in a pulse makes it very interesting for single-photon generation as it can demonstrate single-photon emission without a correlation measurement.

8. Applications of single-photon sources

Single-photon generation on demand is still an end on its own and very few experiments have been realized up to now that rely on single photons. As single photon emitting devices based on single quantum dots are further developed, experiments making use of single photons will be enabled. Here we outline some experiments requiring good single-quantum emitters.

8.1. Quantum cryptography

Applications of single-photon generation on demand to quantum cryptography have been perfomed with single InAs quantum dots in GaAs [102] and with single NV centres in diamond [101]. In quantum cryptography, it is essential that exact single photons are used to guarantee that the transmitted information cannot be eavesdropped. Attenuated laser pulses which are usually used in quantum cryptography experiments are only bad substitutes to true single photons. To ensure that two (or more) photons are almost never sent in a single laser pulse, the attenuated laser beam must be so weak that most pulses will contain no photon at all. Single quantum dot devices will probably find a niche in quantum cryptography.

8.2. Coherence length

The requirement for the implementation of a quantum computation scheme by Knill *et al* [99] based on linear optics and on single-photon emitters is a long coherence source of single photons; ideally the coherence length of photons should be Fourier-limited. A key experiment in this field was reported by Santori *et al* [100] where two succesive single photons emitted by a single quantum dot were overlapped on a beam splitter.

Fourier spectrocopy enables one to reach very high resolutions without incurring large losses. This is of particular interest since the emission linewidth of single quantum dots is very narow, e.g. Gammon *et al* [75] have reported an exciton emission linewidth of 23 μeV for single

GaAs quantum dots in AlGaAs. Bayer and Forchel reported a linewidth of 15 μeV [76] for single InGaAs quantum dots in GaAs. The typical lifetime of the order of a ns for exciton recombinations in III–V quantum dots translates into an expected linewidth of a few μeV. Moreover, a precise measurement of the lineshape requires an even higher resolution. Fourier spectroscopy on single InP dots is reported in the paper by Aichele *et al* in this special issue. We mention that an additional advantage of Fourier spectroscopy is that there are no losses due to blocking by an entrance slit and diffraction into higher diffraction orders.

8.3. Spectral tuning

Because the exact emission energy for a particular quantum dot is random, a method to tune the emission energy would be highly desirable. Stark-shift modulation has been demonstrated on InAs/GaAs quantum dots [84]. The simplest tuning technique is to modify the temperature. The bandgap changes with the temperature, but the intensity of the emission decreases with increasing temperature, the temperature can enable a shift of about 3 meV at the expense of modifications of the intensity and linewidth of the emission.

8.4. Entangled photon pair generation

We have seen that single quantum dots can generate photon pairs through the biexciton–exciton cascade. Benson *et al* [85] suggested that the biexciton and exciton emissions might be entangled in polarization. This entanglement would stem from the spin of the biexciton. We have performed correlation experiments on the combined exciton–biexciton emission from a single InAs quantum dot. Figure 17(a) shows a spectrum taken under pulsed excitation, the excitation power was adjusted so that the exciton and biexciton intensities have the same integrated intensity.

Polarizers were added to each arm of the Hanbury-Brown and Twiss interferometer and correlations were measured for different relative angles between the polarizers. Polarization entanglement is expected to show up as an antibunching dip down to 0 when the two polarizers are set in parallel since only one of the two photons could make its way across the polarizers in this configuration. When the two polarizers are set perpendicular to each other, the antibunching dip should reach a minimum value of 0.5 since the two photons will be transmitted by the polarizers. This polarization correlation must be observed in any base to demonstrate entanglement. Our results are shown in figure 17(b) and only a minute decrease of the antibunching dip was observed for parallel polarizers. The geometry of the quantum dot and the dephasing mechanisms of the excitons must be studied and controlled to generate entangled photon pairs with single quantum dots.

9. Conclusions

We have shown that single quantum dots are well suited for the generation of nonclassical states of light such as single photons, photon pairs and photon triplets. Novel devices based on single quantum dots such as microcavities are now being developed.

Acknowledgments

We acknowledge Werner Seifert from Lund University for providing us with InP quantum dot samples. We are grateful to Roman Sobolewski and Aleksander Verevkin at Rochester

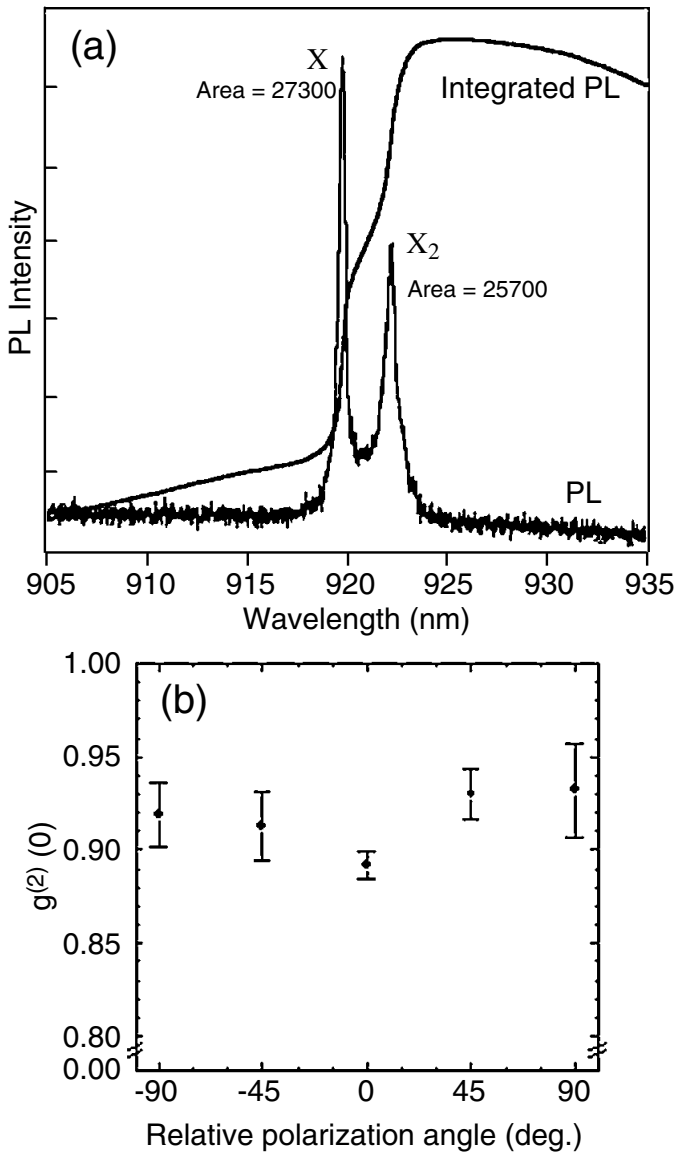

Figure 17. (a) Spectrum taken on a single InAs dot under pulsed excitation. The integral shows that the two emissions have the same intensity. (b) Value of the correlation at $t = 0$.

University for introducing us to superconducting detectors. VZ acknowledges H de Riedmatten and H Zbinden from Geneva University and I Prochazka from the Czech Technical University for discussions on semiconductor detectors. S Fält and J Persson are acknowledged for help with experiments. M Baier and A Malko at EPFL are acknowledged for useful discussions.

References

[1] Scully M O and Zubairy M S 1997 *Quantum Optics* (Cambridge: Cambridge University Press)
[2] Hanbury-Brown R and Twiss R Q 1956 *Nature* **177** 27
[3] Stranski I N and Krastanow L 1938 *Stizungsberichte d. mathem.-naturw.* Kl., Abt. IIb **146** 797

[4] Goldstein L, Glas F, Marzin J Y, Charasse M N and Le Roux G 1985 *Appl. Phys. Lett.* **47** 1099
[5] Petroff P M, Lorke A and Imamoglu A 2001 *Phys. Today* **54** 46
[6] Barnes W L, Björk G, Gérard J M, Jonsson P, Wasey J A E, Worthing P T and Zwiller V 2002 *Eur. Phys. J.* D **18** 197
[7] Mansfield S M and Kino G S 1990 *Appl. Phys. Lett.* **57** 2615
[8] Poweleit C D, Gunther A, Goodnick S and Menéndez J 1998 *Appl. Phys. Lett.* **73** 2275
[9] Sasaki T, Baba M, Yoshita M and Akiyama H 1997 *Japan. J. Appl. Phys.* **36** 962
[10] Vollmer M, Giessen H, Stolz W, Rühle W W, Ghislain L and Elings V 1999 *Appl. Phys. Lett.* **74** 1791
[11] Wu Q, Ghislain L P and Elings V B 2000 *Proc. IEEE* **88** 1491
[12] Yoshita M, Sasaki T, Baba M and Akiyama H 1998 *Appl. Phys. Lett.* **73** 635
[13] Yoshita M, Baba M, Koshiba S, Sakaki H and Akiyama H 1998 *Appl. Phys. Lett.* **73** 2965
[14] Baba M, Yoshita M, Sasaki T and Akiyama H 1999 *Opt. Rev.* **6** 257
[15] Wu Q, Feke G D, Grober R D and Ghislain L P 1999 *Appl. Phys. Lett.* **75** 4064
[16] Koyama K, Yoshita M, Baba M, Suemoto T and Akiyama H 1999 *Appl. Phys. Lett.* **75** 1667
[17] Zhao H, Dal Don B, Moehl S, Kalt H, Ohkawa K and Hommel D 2003 *Phys. Rev.* B **67** 035306
[18] Zhao H, Moehl S and Kalt H 2002 *Appl. Phys. Lett.* **81** 2794
[19] Yoshita M, Koyama K, Haymizu Y, Baba M and Akiyama H 2002 *Japan. J. Appl. Phys.* **41** L858
[20] Yoshita M, Koyama K, Baba M and Akiyama H 2002 *J. Appl. Phys.* **92** 862
[21] Zwiller V and Björk G 2002 *J. Appl. Phys.* **92** 660
[22] Fletcher D A, Crozier K B, Quate C F, Kino G S, Goodson K E, Simanovskii D and Palanker D V 2000 *Appl. Phys. Lett.* **77** 2109
[23] Moehl S, Zhao H, Dal Don B, Wachter S and Kalt H 2003 *J. Appl. Opt.* **93** 6265
[24] Milster T D, Akhvan F, Bailey M, Erwin J K, Felix D M, Hirota K, Koester S, Shimura K and Zhang Y 2001 *Japan. J. Appl. Phys.* **40** 1778
[25] Zhao H, Moehl S, Wachter S and Kalt H 2002 *Appl. Phys. Lett.* **80** 1391
[26] Kimble H J, Dagenais M and Mandel L 1977 *Phys. Rev. Lett.* **39** 691
[27] Moerner W E and Fromm D 2003 *Rev. Sci. Instrum.* **74** 3597
[28] Basche T, Moerner W E, Orrit M and Talon H 1992 *Phys. Rev. Lett.* **69** 1516
[29] Brunel C, Lounis B, Tamarat P and Orrit M 1999 *Phys. Rev. Lett.* **83** 2722
[30] Lounis B and Moerner W E 2000 *Nature* **407** 491
[31] Hettich C, Schmitt C, Zitzmann J, Kühn S, Gerhardt I and Sandoghdar V 2002 *Science* **298** 385
[32] Kitson S C, Jonsson P, Rarity J G and Tapster P R 1998 *Phys. Rev.* A **58** 620
[33] Kurtsiefer C, Mayer S, Zarda P and Weinfurter H 2000 *Phys. Rev. Lett.* **85** 290
[34] Brouri R, Beveratos A, Poizat J-P and Grangier P 2000 *Opt. Lett.* **25** 1294
[35] Beveratos A, Brouri R, Gacoin T, Poizat J-P and Grangier P 2001 *Phys. Rev.* A **64** 061802
[36] Imamoglu A and Yamamoto Y 1992 *Phys. Rev.* B **46** 15982
[37] Imamoglu A and Yamamoto Y 1994 *Phys. Rev. Lett.* **72** 210
[38] Kim J, Benson O, Kan H and Yamamoto Y 1999 *Nature* **397** 500
[39] Samuelson L and Gustafsson A 1995 *Phys. Rev. Lett.* **74** 2395
[40] Gérard J M and Gayral B 2001 *Physica* E **9** 131
[41] Pan J L, McManis J E, Osdachy T, Grober L, Woodall J M and Kindlmann P J 2003 *Nature Mater.* **2** 375
[42] Mirin R P 2004 *Appl. Phys. Lett.* **84** 1260
[43] Michler P, Imamoglu A, Mason M D, Carson P J, Strouse G F and Buratto S K 2000 *Nature* **406** 968
[44] Diedrich F and Walther H 1987 *Phys. Rev. Lett.* **58** 203
[45] von Baeyer H C 2000 *Taming the Atom: the Emergence of the Visible Microworld* (New York: Dover)
[46] Michler P, Kiraz A, Becher C, Schoenfeld W V, Petroff P M, Zhang L, Hu E and Imamoglu A 2000 *Science* **290** 2282
[47] Zwiller V, Blom H, Jonsson P, Panev N, Jeppesen S, Tsegaye T, Goobar E, Pistol M-E, Samuelson L and Björk G 2001 *Appl. Phys. Lett.* **78** 2476

[48] Thompson R M, Stevenson R M, Shields A J, Farrer I, Lobo C J, Ritchie D A, Leadbeater M L and Pepper M 2001 *Phys. Rev.* B **64** 201302
[49] Zwiller V, Jonsson P, Blom H, Jeppesen S, Pistol M-E, Samuelson L, Katznelson A A, Kotelnikov E Y, Evtikhiev V and Björk G 2002 *Phys. Rev.* A **66** 053814
[50] Zwiller V, Aichele T, Seifert W, Persson J and Benson O 2003 *Appl. Phys. Lett.* **82** 1509
[51] Moreau E, Robert I, Manin L, Thierry-Mieg V, Gérard J M and Abram I 2001 *Phys. Rev. Lett.* **87** 183601
[52] Kiraz A, Falth S, Becher C, Gayral B, Schoenfeld W V, Petroff P M, Zhang L, Hu E and Imamoglu A 2002 *Phys. Rev.* B **65** 161303
[53] Schubert E F 2003 *Light-emitting Diodes* (Cambridge: Cambridge University Press)
[54] Landolt-Börnstein 1982 *Semiconductors: Physics of Group IV Elements and III–V Compounds* vol 17a (Berlin: Springer) p 538
[55] Prochazka I, Hamal K and Sopko B 2004 *J. Mod. Opt.* **51** 1289
[56] Kim J, Yamamoto Y and Hogue H H 1997 *Appl. Phys. Lett.* **70** 2852
[57] Rarity J G, Wall T E, Ridley K D, Owens P C M and Tapster P R 2000 *Appl. Opt.* **39** 6746
[58] Yoshizawa A and Tsuchida H 2001 *Japan. J. Appl. Phys.* **40** 200
[59] Ribordy G, Gautier J-D, Zbinden H and Gisin N 1998 *Appl. Opt.* **37** 2272
[60] Bourennane M, Gibson F, Karlsson A, Hening A, Jonsson P, Tsegaye T, Ljunggren D and Sundberg E 1999 *Opt. Express* **4** 383
[61] Shields A J, O'Sullivan M P, Farrer I, Ritchie D A, Hogg R A, Leadbeater M L, Norman C E and Pepper M 2000 *Appl. Phys. Lett.* **76** 3673
[62] Kardynal B E, Shields A J, Beattie N S, Farrer I, Cooper K and Ritchie D A 2004 *Appl. Phys. Lett.* **84** 419
[63] Miller A J, Nam S W, Martinis J M and Sergienko A V 2003 *Appl. Phys. Lett.* **83** 791
[64] Sebald K, Michler P, Passow T, Hommel D, Bacher G and Forchel A 2002 *Appl. Phys. Lett.* **81** 2920
[65] Aichele T, Zwiller V, Benson O, Akimov I and Henneberger F 2003 *J. Opt. Soc. Am.* B **20** 2189
[66] Ulrich S M, Strauf S, Michler P, Bacher G and Forchel A 2003 *Appl. Phys. Lett.* **83** 1848
[67] Moriwaki O, Someya T, Tachibana K, Ishida S and Arakawa Y 2000 *Appl. Phys. Lett.* **76** 2361
[68] Robinson J W, Rice J H, Jarjour A, Smith J D, Taylor R A, Oliver R A, Briggs G A D, Kappers M J, Humphreys C J and Arakawa Y 2003 *Appl. Phys. Lett.* **83** 2674
[69] Oliver R A, Briggs G A D, Kappers M J, Humphreys C J, Yasin S, Rice J H, Smith J D and Taylor R A 2003 *Appl. Phys. Lett.* **83** 755
[70] Kaiser S, Mensing T, Worschech L, Klopf F, Reithmaier J P and Forchel A 2002 *Appl. Phys. Lett.* **81** 4898
[71] Ward M B, Unitt D C, Yuan Z, See P, Stevenson R M, Cooper K, Atkinson P, Farrer I, Ritchie D A and Shields A J 2004 *Physica* E **21** 390
[72] Zwiller V, Zinoni C, Buchs G, Alloing B and Fiore A 2004 to be submitted
[73] http://www.idquantique.com/
[74] http://www.magiqtech.com/index.php
[75] Gammon D, Snow E S, Shanabrook B V, Katzer D S and Park D 1996 *Science* **273** 87
[76] Bayer M and Forchel A 2002 *Phys. Rev.* B **65** 041308
[77] Ostermayer F W, Kohl P A and Burton R H 1983 *Appl. Phys. Lett.* **43** 642
[78] Kim Y-S, Kim J, Choe J-S, Roh Y-G, Jeon H and Woo J C 2000 *IEEE Photon. Technol. Lett.* **12** 507
[79] Zrenner A 2000 *J. Chem. Phys.* **112** 7790
[80] Gustafsson A, Pistol M-E, Montelius L and Samuelson L 1998 *J. Appl. Phys.* **84** 1715
[81] Baier M, Pelucchi E, Kapon E, Varoutsis S, Gallart M, Robert-Philip I and Abram I 2004 *Appl. Phys. Lett.* **84** 648
[82] Panev N, Persson A I, Sköld N and Samuelson L 2003 *Appl. Phys. Lett.* **83** 2238
[83] Hours J, Varoutsis S, Gallart M, Bloch J, Robert-Philip I, Cavanna A, Abram I, Laruelle F and Gérard J M 2003 *Appl. Phys. Lett.* **82** 2206
[84] Alén B, Bickel F, Karrai K, Warburton R J and Petroff P M 2003 *Appl. Phys. Lett.* **83** 2235
[85] Benson O, Santori C, Pelton M and Yamamoto Y 2000 *Phys. Rev. Lett.* **84** 2513
[86] Jeppesen S, Miller M, Hessman D, Kowalski B, Maximov I and Samuelson L 1996 *Appl. Phys. Lett.* **68** 2228

[87] An H and Motohisa J 2000 *Appl. Phys. Lett.* **77** 385
[88] Ishikawa T, Kohmoto S and Asakawa K 1998 *Appl. Phys. Lett.* **73** 1712
[89] Konkar A, Rajkumar K C, Xie Q, Chen P, Madhukar A, Lin H T and Rich D H 1995 *J. Crystal Growth* **150** 311
[90] Yuan Z, Kardynal B E, Stevenson R M, Shields A J, Lobo C J, Cooper K, Beattie N S, Ritchie D A and Pepper M 2002 *Science* **295** 102
[91] Vahala K J 2003 *Nature* **424** 839
[92] Landin L, Borgström M, Kleverman M, Pistol M-E, Samuelson L, Seifert W and Zhang X H 2000 *Thin Solid Films* **364** 161
[93] Il'in K S, Milostnaya I I, Verevkin A A, Gol'tsman G N, Gershenzon E M and Sobolewski R 1998 *Appl. Phys. Lett.* **73** 3938
[94] Gol'tsman G, Okunev O, Chulkova G, Lipatov A, Dzardanov A, Smirnov K, Semonov A, Voronov B, Williams C and Sobolewski R 2001 *IEEE Trans. Appl. Supercond.* **11** 574
[95] Lipatov A *et al* 2002 *Supercond. Sci. Technol.* **15** 1689
[96] Gol'tsman G N, Smirnov K, Kouminov P, Voronov B, Kaurova N, Drakinsky V, Zhang J, Verevkin A and Sobolewski R 2003 *IEEE Trans. Appl. Supercond.* **13** 192
[97] Zhang J, Slysz W, Verevkin A, Okunev O, Chulkova G, Korneev A, Lipatov A, Gol'tsman G N and Sobolewski R 2003 *IEEE Trans. Appl. Supercond.* **13** 180
[98] Korneev A *et al* 2004 submitted
[99] Knill E, Laflamme R and Milburn G J 2001 *Nature* **409** 46
[100] Santori C, Fattal D, Vuĉković J, Solomon G S and Yamamoto Y 2002 *Nature* **419** 594
[101] Beveratos A, Brouri R, Gacoin T, Villing A, Poizat J-P and Grangier P 2002 *Phys. Rev. Lett.* **89** 187901
[102] Waks E, Inoue K, Santori C, Fattal D, Vuckovic J, Solomon G S and Yamamoto Y 2002 *Nature* **420** 762